MAGNETOHYDRODYNAMIC FLOW OF NANOFLUID OVER PERMEABLE STRETCHING SHEET WITH CONVECTIVE BOUNDARY CONDITIONS

by

Tasawar HAYAT [a,b], ***Maria IMTIAZ*** [a*], ***and Ahmed ALSAEDI*** [b]

[a] Department of Mathematics, Quaid-I-Azam University, Islamabad, Pakistan
[b] NAAM Research Group, Department of Mathematics, Faculty of Science, King Abdulaziz University, Jeddah, Saudi Arabia

Original scientific paper
DOI: 10.2298/TSCI140819139H

Analysis has been carried out for the magnetohydrodynamic boundary layer flow of nanofluid. The flow is caused by a permeable stretching sheet. Convective type boundary conditions are employed in modeling the heat and mass transfer process. Appropriate transformations reduce the non-linear partial differential equations to ordinary differential equations. The convergent series solutions are constructed. Graphical results of different parameters are discussed. The behaviors of Brownian motion and thermophoretic diffusion of nanoparticles have been examined. The dimensionless expressions of local Nusselt and local Sherwood numbers have been evaluated and discussed.

Key words: *magnetohydrodynamic nanofluid, suction/injection, convective boundary conditions*

Introduction

In recent times, the convective heat transfer through nanoparticles has been the topic of extensive research. The nanoparticles (nanometer sized particles) are made up of metals, carbides, oxides, or carbon nanotubes. The nanofluids are formed by adding nanoparticles into many conventional fluids like water, ethylene glycol, and engine oil. The use of additive is a process which enhances the heat transfer performance of base fluids. Choi [1] experimentally found that addition of nanoparticles in conventional/base fluid appreciably enhances the thermal conductivity of the fluid. Cooling is one of the technical challenges faced in many industries. Use of nanofluids as coolants allows for smaller size and better positioning of the radiators which eventually consumes less energy for overcoming resistance on the road. Nanoparticles in refrigerant/lubricant mixtures could enable a cost effective technology for improving the efficiency of chillers that cool buildings. Analysis of fluid flow in presence of magnetic field has promising applications in engineering, chemistry, physics, polymer industry, and metallurgy. Rate of heat cooling has key role in improving the desired characteristics of end product in such applications. An electrically conducting fluid subject to magnetic field is useful in controlling the rate of cooling. The magnetohydrodynamic (MHD) flow is also of great interest in problems associated with physiological fluids, for instance, blood plasma and blood pump machines.

* Corresponding author; e-mail: mi_qau@yahoo.com

Having such salient features in mind, numerous articles have been written for the MHD flows in different flow configurations. The MHD nanofluids are further important in hyperthermia, cancer therapy, and safer surgery by cooling sink float separation, magnetic cell separation, and contrast enhancement in magnetic resonance imaging. At present, the literature on theoretical and experimental attempts about nanofluids is quite extensive. The comprehensive review on nanofluids can be found in [2-8]. Detailed review on this topic up to 2012 has been made recently in [9, 10]. Besides these, a comprehensive survey of convective transport in nanofluids is presented by Buongiorno [11]. He developed a non-homogeneous equilibrium model for convective transport to describe the heat transfer enhancement of nanofluids. Such abnormal increase in thermal conductivity occurs due to the presence of two main velocity-slip effects, namely, the Brownian diffusion and the thermophoretic diffusion of the nanoparticles. Later, Buongiorno *et al.* [12] conducted novel investigations which show no anomalous thermal conductivity enhancement in the considered fluids. Some recent research articles on the topic can be seen through the studies, [13-23] and many refs. therein.

In the polymer industry, the flow over a stretching surface has important applications. Glass blowing, continuous casting and spinning of fibres also involve the flow due to stretching surface. Crane [24] provided the classical solution for the boundary layer flow of viscous fluid over a sheet moving with velocity varying linearly with distance from a fixed point. The classical work of Crane [24] has been undertaken for the stretching flows in different configurations. Mukhopadhyay [25] investigated the slip effects on MHD boundary layer flow by an exponentially stretching sheet with suction/blowing and thermal radiation. Effects of thermal radiation on micropolar fluid flow and heat transfer over a porous shrinking sheet have been investigated by Bhattacharyya *et al.* [26]. Exact solutions for 2-D laminar flow over a continuously stretching or shrinking sheet in an electrically conducting quiescent couple stress fluid have been derived by Turkyilmazoglu [27]. Turkyilmazoglu [28] presented a note on micropolar fluid flow and heat transfer over a porous shrinking sheet. Effect of heat transfer in flow of nanofluids over a permeable stretching wall in a porous medium is analyzed by Sheikholeslami *et al.* [29]. Sheikholeslami and Ganji [30] discussed the 3-D flow of nanofluid in a rotating system. Ibrahim *et al.* [31] analyzed the MHD stagnation point flow of nanofluid towards a stretching sheet. Effect of slip on unsteady stagnation point flow of nanofluid over a stretching sheet is investigated by Malvandi *et al.* [32].

The purpose of present paper is to examine the nanofluid flow over a stretching surface by homotopy analysis method (HAM) [33-39]. The surface is taken permeable and exhibits convective type boundary conditions [40, 41]. In fact the nanoparticles are used to enhance the thermal conductivity of the fluid. On the other hand the convective boundary condition in dimensionless form is appeared as Biot number. Increase in Biot number give rise to the temperature. Increase in temperature corresponds to an enhancement in the thermal conductivity. So the nanofluid with convective boundary condition is more appropriate model in comparison to the constant surface temperature conditions. Convective boundary conditions represent the heat transfer rate through the surface being proportional to the local difference in temperature with the ambient conditions. Such configuration occurs in several engineering devices for instance in heat exchangers, where the conduction in the solid tube wall is greatly influenced by the condition in the fluid flowing over it.

Mathematical analysis

We consider the 2-D flow of nanofluid bounded by a permeable stretching sheet. The x-axis is taken along the stretching surface in the direction of motion, and y-axis is perpendicular to it. A uniform transverse magnetic field of strength, B_0, is applied parallel to the y-axis. It is assumed that the effects of induced magnetic and electric fields are negligible. Salient features of Brownian motion and thermophoresis are present. The temperature, T, and the nanoparticle fraction, C, at the surface have constant values T_w and C_w, respectively. The ambient values of T and C attained as y tends to infinity are denoted by T_∞ and C_∞, respectively. The conservation of mass, momentum, energy, and nanoparticles equations for nanofluids are:

$$\frac{\partial u}{\partial x}+\frac{\partial v}{\partial y}=0 \tag{1}$$

$$u\frac{\partial u}{\partial x}+v\frac{\partial u}{\partial y}=\nu\frac{\partial^2 u}{\partial y^2}-\frac{\sigma B_0^2 u}{\rho_\mathrm{f}} \tag{2}$$

$$u\frac{\partial T}{\partial x}+v\frac{\partial T}{\partial y}=\alpha\frac{\partial^2 T}{\partial y^2}+\tau\left[D_\mathrm{B}\frac{\partial C}{\partial y}\frac{\partial T}{\partial y}+\frac{D_\mathrm{T}}{T_\infty}\left(\frac{\partial T}{\partial y}\right)^2\right] \tag{3}$$

$$u\frac{\partial C}{\partial x}+v\frac{\partial C}{\partial y}=D_\mathrm{B}\frac{\partial^2 C}{\partial y^2}+\frac{D_\mathrm{T}}{T_\infty}\frac{\partial^2 T}{\partial y^2} \tag{4}$$

where u and v are the velocity components along the x- and y-directions, respectively, ρ_f is the fluid density, ν – the kinematic viscosity, $(\rho c)_\mathrm{f}$ – the heat capacity of the fluid, $\tau=(\rho c)_p/(\rho c)_\mathrm{f}$ – the ratio between the effective heat capacity of the nanoparticle material and heat capacity of the fluid, D_B – the Brownian diffusion coefficient, D_T – the thermophoretic diffusion coefficient, α – the thermal diffusivity, σ – the electrical conductivity of the base fluid, and c_p – the specific heat at constant pressure.

We assume the bottom surface of the plate is heated by convection from a hot fluid at temperature, T_f, which provides a heat transfer coefficient, h. The boundary conditions are prescribed:

$$u=u_w(x)=ax,\ \ v=v_\mathrm{w},\ \ -k\frac{\partial T}{\partial y}=h(T_\mathrm{f}-T),\ \ -D_\mathrm{m}\frac{\partial C}{\partial y}=k_\mathrm{m}(C_\mathrm{f}-C)\quad \text{at } y=0,$$
$$u=0,\ T\to T_\infty,\ C\to C_\infty\ \text{ as } y\to\infty \tag{5}$$

in which v_w is the wall heat transfer velocity, k – the thermal conductivity of fluid, h – the convective heat transfer coefficient, D_m – the molecular diffusivity of the species concentration, and k_m – the wall mass transfer coefficient. Using the transformations:

$$\eta=\sqrt{\frac{a}{\nu}}y,\quad u=axf'(\eta),\quad v=-\sqrt{\nu a}f(\eta),\quad \theta(\eta)=\frac{T-T_\infty}{T_\mathrm{f}-T_\infty},\quad \phi(\eta)=\frac{C-C_\infty}{C_\mathrm{f}-C_\infty} \tag{6}$$

eq. (1) is satisfied automatically, and eqs. (2)-(5) take the forms:

$$f'''-f'^2+ff''-\mathrm{M}f'=0 \tag{7}$$

$$\frac{1}{\mathrm{Pr}}\theta''+f\theta'+N_\mathrm{B}\phi'\theta'+N_\mathrm{T}\theta'^2=0 \tag{8}$$

$$\phi''+\mathrm{Sc}\,f\phi'+\frac{N_\mathrm{T}}{N_\mathrm{B}}\theta''=0 \tag{9}$$

$$f(0)=S, \qquad f'(0)=1, \qquad \theta'(0)=-\gamma_1[1-\theta(0)], \qquad \phi'(0)=-\gamma_2[1-\phi(0)],$$
$$f'(\infty)=0, \qquad \theta(\infty)=0, \qquad \phi(\infty)=0 \tag{10}$$

where prime indicates the differentiation with respect to η. Moreover, Prandtl number, thermal Biot number, γ_1, concentration Biot number, γ_2, mass transfer parameter, S with $S>0$ for suction, and $S<0$ for injection, Schmidt number, Hartman number, Brownian motion parameter, N_B, and thermophoresis parameter, N_T, are defined by the definitions:

$$\mathrm{Pr}=\frac{\nu}{\alpha}, \qquad \gamma_1=\frac{h}{k}\sqrt{\frac{\nu}{a}}, \qquad \gamma_2=\frac{k_\mathrm{m}}{D_\mathrm{m}}\sqrt{\frac{\nu}{a}}, \qquad S=-\frac{v_\mathrm{w}}{\sqrt{\nu a}}, \qquad \mathrm{Sc}=\frac{\nu}{D_\mathrm{B}}, \qquad \mathrm{M}=\frac{\sigma B_0^2}{\rho_\mathrm{f} a},$$
$$N_\mathrm{B}=\frac{(\rho c)_p D_\mathrm{B}(C_\mathrm{w}-C_\infty)}{(\rho c)_\mathrm{f}\nu}, \qquad N_\mathrm{T}=\frac{(\rho c)_p D_\mathrm{T}(T_\mathrm{w}-T_\infty)}{(\rho c)_\mathrm{f} T_\infty \nu} \tag{11}$$

The local Nusselt number, Nu, and Sherwood number, Sh, are:

$$\mathrm{Nu}=\frac{xq_\mathrm{w}}{k(T_\mathrm{f}-T_\infty)}, \qquad \mathrm{Sh}=\frac{xq_\mathrm{m}}{D_\mathrm{B}(C_\mathrm{f}-C_\infty)} \tag{12}$$

where q_w and q_m denote the wall heat and mass fluxes, respectively. In dimensionless form:

$$\mathrm{NuRe}_x^{-1/2}=-\theta'(0), \qquad \mathrm{ShRe}_x^{-1/2}=-\phi'(0) \tag{13}$$

where $\mathrm{Re}_x=u_w(x)x/\nu$ is the local Reynolds number.

We choose the initial guesses $f_0(\eta)$, $\theta_0(\eta)$ and $\phi_0(\eta)$ and the linear operators $\mathbf{L}_\mathrm{f}$, $\mathbf{L}_\theta$ and $\mathbf{L}_\phi$ in the forms:

$$f_0(\eta)=S+1-\exp(-\eta) \tag{14}$$

$$\theta_0(\eta)=\frac{\gamma_1}{1+\gamma_1}\exp(-\eta) \tag{15}$$

$$\phi_0(\eta)=\frac{\gamma_2}{1+\gamma_2}\exp(-\eta) \tag{16}$$

$$\mathbf{L}_\mathrm{f}(f)=f'''-f' \tag{17}$$

$$\mathbf{L}_\theta(\theta)=\theta''-\theta \tag{18}$$

$$\mathbf{L}_\phi(\phi)=\phi''-\phi \tag{19}$$

where the convergence depends upon the non-zero auxiliary parameters $\hbar_\mathrm{f}$, $\hbar_\theta$, and $\hbar_\phi$.

Analysis of the results

Convergence of the derived series solutions

The solution of problem contained in eqs. (7)-(10) is computed employing HAM. The convergence region and rate of approximations for the functions f, θ, and ϕ can be controlled and adjusted through the auxiliary parameters $\hbar_\mathrm{f}$, $\hbar_\theta$, and $\hbar_\phi$ (tab. 1). For the admissible values of $\hbar_\mathrm{f}$, $\hbar_\theta$, and $\hbar_\phi$, the $\hbar$-curves of $f''(\eta)$, $\theta'(\eta)$, and $\phi'(\eta)$ for 14th order of approximations are displayed. Figure 1 shows that the admissible values of $\hbar_\mathrm{f}$ is

$-1.5 \le \hbar_f \le -0.4$. Figure 2 displays that the range for θ is $-1.7 \le \hbar_\theta \le -0.6$, and similarly for ϕ is $-1.6 \le \hbar_\phi \le -0.7$. Further, the series solutions converge in the whole region of η when $\hbar_f = \hbar_\theta = \hbar_\phi = -1.2$.

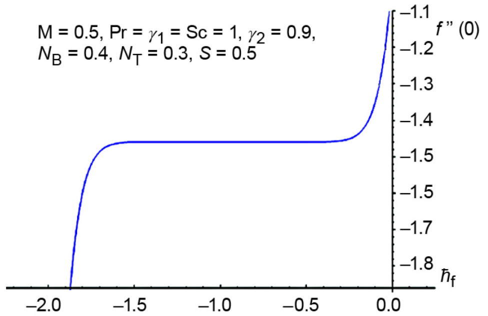

Figure 1. The $\hbar$-curve for f

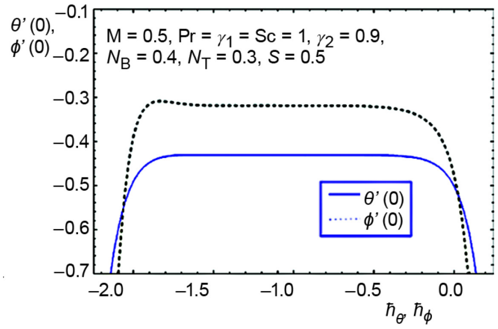

Figure 2. The $\hbar$-curve for θ and ϕ

Results and discussion

The effects of various parameters on the velocity, temperature, and concentration profiles are discussed. Figures 3 and 4 are plotted to show the effects of Hartman number and mass transfer parameter, S, on the velocity profile, f'. Figure 3 shows the effects of Hartman number on f'. Application of magnetic field has the tendency to slow down the movement of the fluid particles and consequently the velocity decreases. Figure 4 displays the effect of S on f'. In this figure the velocity field f' decreases when S increases. In fact applying suction leads to draw the amount of fluid particles into the wall and hence the velocity boundary layer decreases.

Effects of the Brownian motion parameter, N_B, thermophoresis parameter, N_T, Schmidt number, Prandtl number, Hartman number, mass transfer parameter, S, thermal Biot number, γ_1, and concentration Biot number, γ_2, on the temperature profile, θ, and the concentration profile, ϕ, are shown in figs. 5-9. It is noted that an increase in the Brownian motion parameter, N_B, thermophoresis parameter, N_T, and Schmidt number, increase the temperature profile, θ, as shown in figs. 5-7. The effects of Prandtl number, on the temperature profile are depicted in fig. 8. This graph shows that the temperature profile θ, decreases

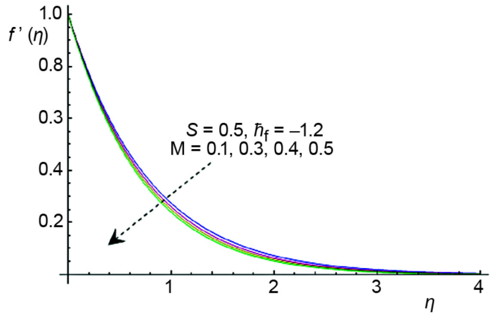

Figure 3. Influence of M on f'

Table 1. Convergence of HAM solutions for different order of approximations when N_B = 0.4, N_T = 0.3, Sc = 1, Pr = 1, M = 0.4, S = 0.5, γ_1 = 1, and γ_2 = 0.9

Order of approximations	$-f''(0)$	$-\theta'(0)$	$-\phi'(0)$
1	1.54000	0.441053	0.344668
5	1.45883	0.431349	0.319776
10	1.45934	0.430920	0.318765
15	1.45934	0.430912	0.318750
20	1.45934	0.430912	0.318750
25	1.45934	0.430912	0.318750
30	1.45934	0.430912	0.318750
35	1.45934	0.430912	0.318750
40	1.45934	0.430912	0.318750
50	1.45934	0.430912	0.318750
60	1.45934	0.430912	0.318750

when Prandtl number increases. In fact, the thermal diffusivity decreases by increasing Prandtl number and thus the heat diffused away slowly from the heated surface. Figure 9 illustrates the effects of Hartman number on temperature profile θ. The Lorentz force is a resistive force which opposes the fluid motion. As a sequence the heat is produced and thus thermal boundary layer thickness increases. Further, the temperature profile θ decreases when S is increased, fig. 10. The temperature profile θ also increases when the thermal Biot number, γ_1, increases (fig. 11). Figure 12 illustrates the effects of N_B on ϕ. The concentration profile, ϕ, decreases by increasing the Brownian motion parameter, N_B. Influence of N_T on ϕ can be seen in fig. 13. There is an increase in ϕ when N_T is increased. Figures 14-17 display the effects of Schmidt number, Prandtl number, Hartman number, and S on the concentration profile ϕ. It is observed that concentration profile, ϕ, decreases by increasing these parameters.

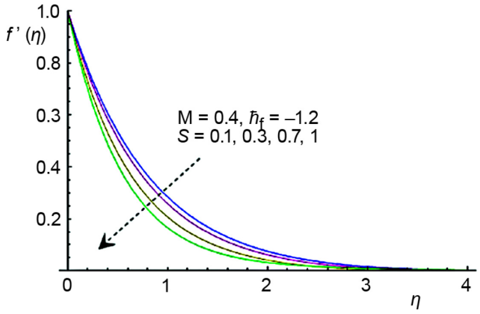

Figure 4. Influence of S on f'

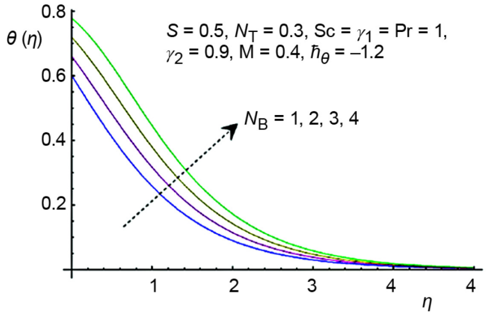

Figure 5. Influence of N_B on θ

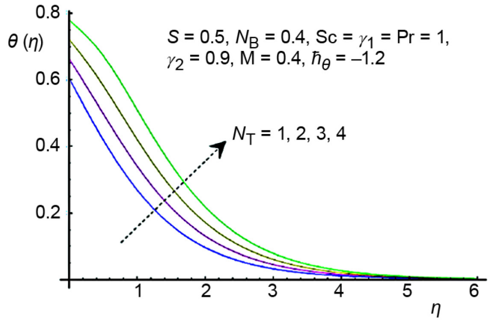

Figure 6. Influence of N_T on θ

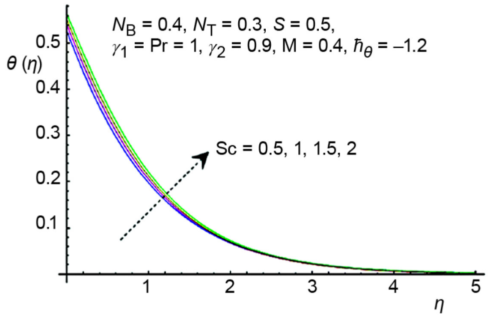

Figure 7. Influence of Sc on θ

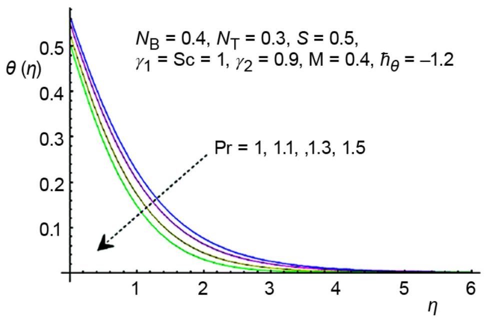

Figure 8. Influence of Pr on θ

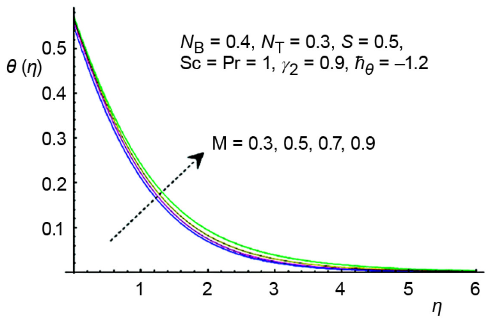

Figure 9. Influence of M on θ

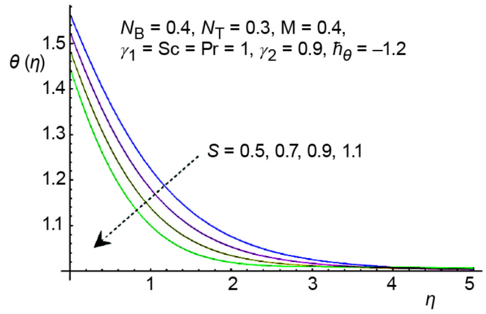

Figure 10. Influence of *S* on θ

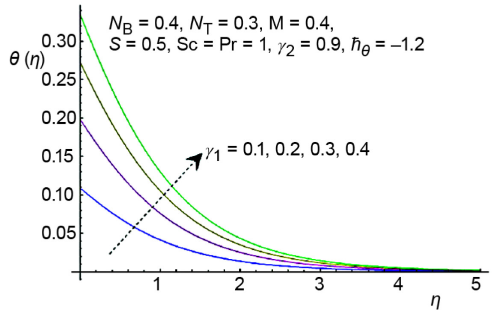

Figure 11. Influence of γ_1 on θ

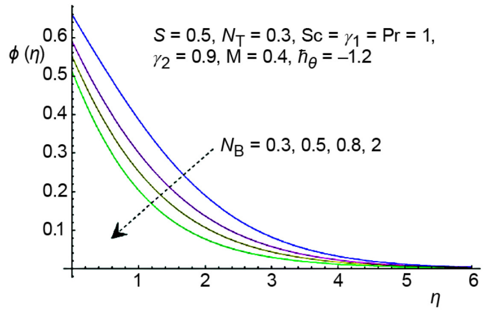

Figure 12. Influence of N_B on ϕ

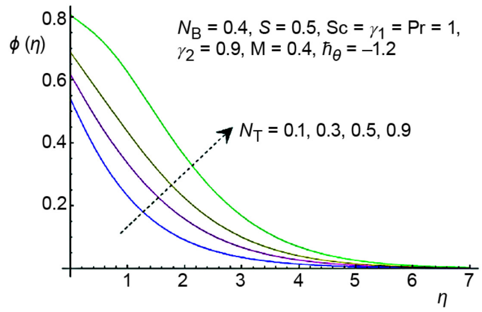

Figure 13. Influence of N_T on ϕ

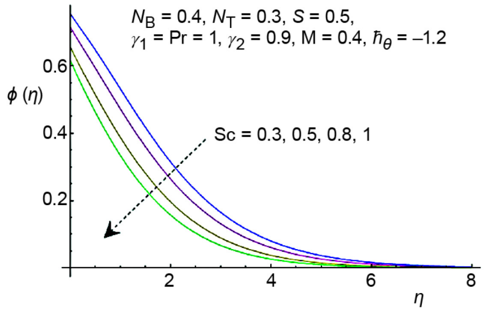

Figure 14. Influence of Sc on ϕ

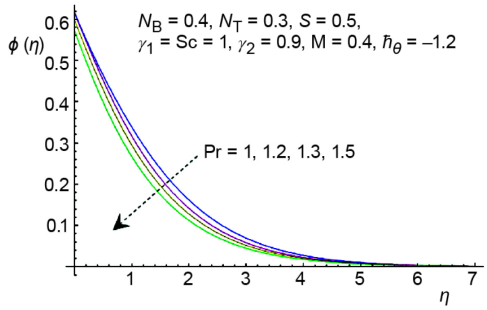

Figure 15. Influence of Pr on ϕ

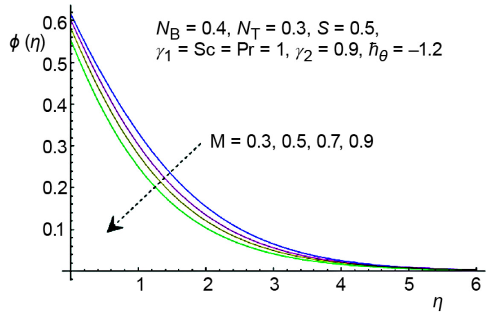

Figure 16. Influence of M on ϕ

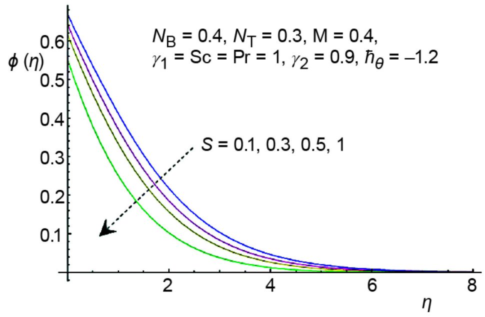

Figure 17. Influence of *S* on ϕ

It is observed from fig. 18 that the mass fraction field ϕ, increases when thermal Biot number, γ_1, is increased. Also the concentration profile, ϕ, increases by increasing concentration Biot number, γ_2, as depicted in fig. 19.

Figures 20 and 21 describe the variations of the Nusselt number $\mathrm{Nu}(\mathrm{Re}_x)^{-1/2}$ for N_B, N_T, and Scmidt number. It is noticed that heat transfer rate decreases as N_B and N_T increase for Scmidt number. Figure 22 shows the effects of γ_1 and S on the Nusselt number. In this figure, heat transfer rate increases as γ_1 increases for S. Figures 23 and 24 illustrate the variation in dimensionless mass transfer rate $\mathrm{Sh}(\mathrm{Re}_x)^{-1/2}$ *vs.* N_B and N_T. Here, the mass transfer rate increases with an increas in N_B and decreases with an increase in N_T. Effects of γ_2 and mass transfer parameter S on the Scmidt numberare displayed in fig. 25. It is noted that mass transfer rate increases for higher γ_2.

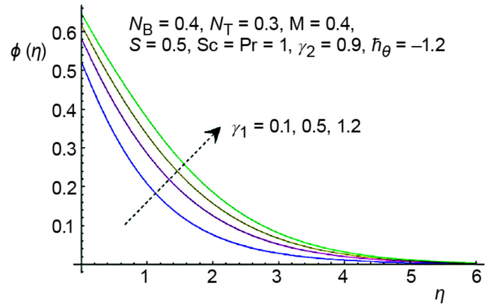

Figure 18. Influence of γ_1 on ϕ

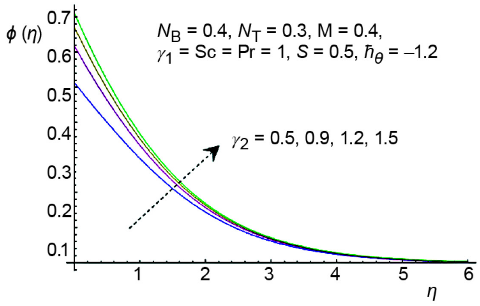

Figure 19. Influence of γ_2 on ϕ

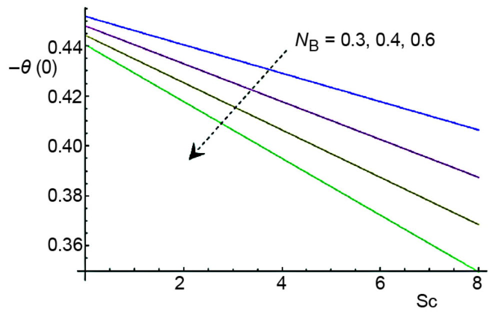

Figure 20. Effects of N_B and Sc on $-\theta'(0)$

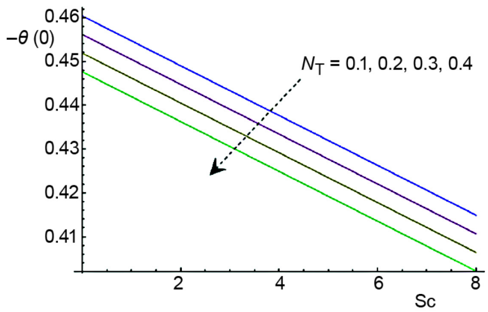

Figure 21. Effects of N_T and Sc and on $-\theta'(0)$

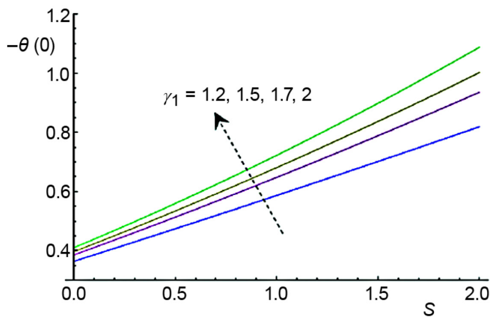

Figure 22. Effects of γ_1 and S on $-\theta'(0)$

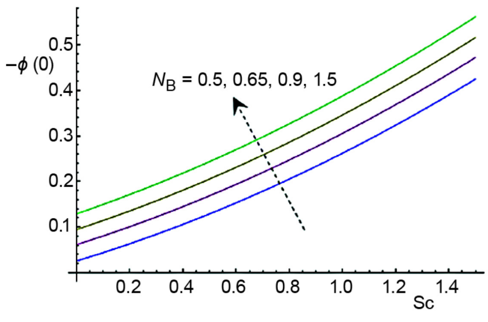

Figure 23. Effects of N_B and Sc and on $-\phi'(0)$

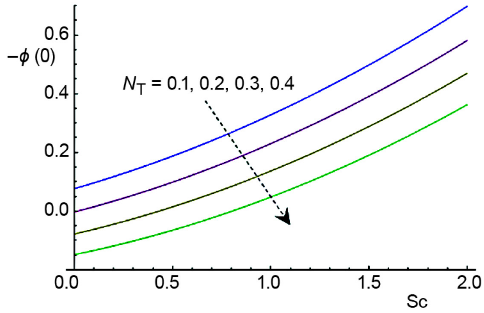

Figure 24. Effects of N_T and Sc on $-\phi'(0)$

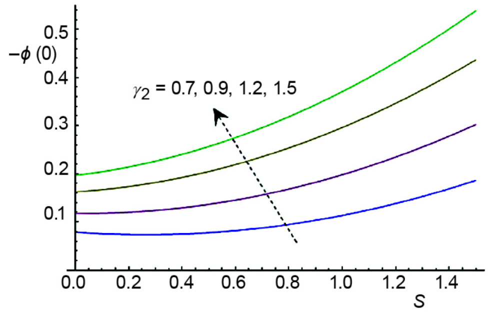

Figure 25. Effects of γ_2 and S and on $-\phi'(0)$

Conclusions

The flow of nanofluid generated by a permeable stretching sheet is studied. Effects of different parameters on the velocity, temperature, and concentration distributions are explored. The following observations are worth mentioning.

- The effects of Hartman number and S are similar on the velocity profile f'.
- Increase in N_B, N_T, Schmidt number, M, and γ_1 enhances the temperature profile while increase in Prandtl number and S decreases the temperature profiles.
- There is enhancement of concentration for increasing N_T, γ_1, and γ_2.
- Local Nusselt number increases by larger γ_1.
- Local Sherwood number increases by increasing N_B and γ_2.

Nomenclature

a – stretching constant, [s^{-1}]
B_0 – uniform magnetic field strength, [kgs^{-1}A^{-1}]
C – concentration
C_∞ – ambient fluid concentration
C_f – convective fluid concentration
c_p – specific heat, [m^{2}s^{-2}]
D_B – Brownian diffusion coefficient, [kgm^{-1}s^{-1}]
D_m – molecular diffusivity of the species concentration
D_T – thermophoretic diffusion coefficient, [kgm^{-1}s^{-1}K^{-1}]
h – convective heat transfer coefficient, [WK^{-1}m^{-2}]
k – thermal conductivity, [WK^{-1}m^{-1}]
k_m – wall mass transfer coefficient
M – Hartman number
N_B – Brownian motion parameter
N_T – thermophoresis parameter
Nu – local Nusselt number
Pr – Prandtl number
q_m – surface mass flux, [Wm^{-2}]
q_w – surface heat flux, [Wm^{-2}]
Re$_x$ – local Reynolds number
S – mass transfer parameter
Sc – Schmidt number
Sh – local Sherwood number
T – temperature, [K]
T_∞ – ambient fluid temperature, [K]
T_f – convective fluid temperature, [K]
u, v, – x- and y-direction velocity components, [ms^{-1}]
v_w – wall heat transfer velocity, [ms^{-1}]

Greek symbols

α – thermal diffusivity, [m^{2}s^{-1}]
ρ – density, [kgm^3]
σ – electrical conductivity, [s^{3}A^{2}kg^{-1}m^{-3}]
τ – ratio between the effective heat capacity of the nanoparticles and fluid
ν – kinematic viscosity, [m^{2}s^{-1}]

References

[1] Choi, S. U. S., Enhancing Thermal Conductivity of Fluids with Nanoparticles, *ASME Int. Mech. Eng., 66* (1995), Jan., pp. 99-105
[2] Das, S. K., *et al., Science and Technology,* John Wiley and Sons, N. J., USA, 2007

[3] Daungthongsuk, W., Wongwises, S., A Critical Review of Convective Heat Transfer Nanofluids, *Renew. Sustain. Eng. Rev., 11* (2007), 5, pp. 797-817
[4] Trisaksri, V., Wongwises, S., Critical Review of Heat Transfer Characteristics of Nanofluids, *Renew. Sustain. Eng. Rev., 11* (2007), 3, pp. 512-523
[5] Wang, X. Q., Mujumdar, A. S., Heat Transfer Characteristics of Nanofluids: a Review, *Int. J. Therm. Sci., 46* (2007), 1, pp. 1-16
[6] Wang, X. Q., Mujumdar, A. S., A Review on Nanofluids – Part I: Theoretical and Numerical Investigations, *Brazilian J. Chem. Eng., 25* (2008), 4, pp. 613-630
[7] Wang, X. Q., Mujumdar, A. S., A Review on Nanofluids – Part II: Experiments and Applications, *Brazilian J. Chem. Eng., 25* (2008), 4, pp. 631-648
[8] Kakac, S., Pramuanjaroenkij, A., Review of Convective Heat Transfer Enhancement with Nanofluids, *Int. J. Heat Mass Transfer, 52* (2009), 13-14, pp. 3187-3196
[9] Mohammed, H. A., *et al.,* Heat Transfer and Fluid Flow Characteristics in Microchannels Heat Exchanger Using Nanofluids: A review, *Renew. Sustain. Eng. Rev., 15* (2011), 3, pp. 1502-1512
[10] Dalkilic, A. S., *et al.,* Forced Convective Heat Transfer of Nanofluids: A Review of the Recent Literature, *Current Nanoscience, 8* (2012), 6, pp. 949-969
[11] Buongiorno, J., Convective Transport in Nanofluids, *ASME J. Heat Transf., 128* (2006), 3, pp. 240-250
[12] Buongiorno, J. *et al.*, A Benchmark Study on the Thermal Conductivity of Nanofluids, *J. Appl. Phys. 106* (2009), ID 094312
[13] Turkyilmazoglu, M., Nanofluid Flow and Heat Transfer due to a Rotating Disk, *Computers and Fluids, 94* (2014), 1, pp. 139-146
[14] Turkyilmazoglu, M., Unsteady Convection Flow of Some Nanofluids Past a Moving Vertical Flat Plate with Heat Transfer, *J. Heat Transfer, 136* (2013), 3, ID 031704
[15] Sheikholeslami, M., Ganji, D. D., Heat Transfer of Cu-Water Nanofluid Flow between Parallel Plates, *Powder Technology, 235* (2013), Feb., pp. 873-879
[16] Sheikholeslami, M., *et al.,* Analytical Investigation of MHD Nanofluid Flow in a Semi-Porous Channel, *Powder Technology, 246* (2013), Sep., pp. 327-336
[17] Xu, H., *et al.,* Flow and Heat Transfer in a Nano-Liquid Film over an Unsteady Stretching Surface, *Int. J. Heat and Mass Transfer, 60* (2013), May, pp. 646-652
[18] Rashidi, M. M., *et al.,* Entropy Generation in Steady MHD Flow due to a Rotating Porous Disk in a Nanofluid, *Int. J. Heat and Mass Transfer, 62* (2013), July, pp. 515-525
[19] Niu, J., *et al.,* Slip Flow and Heat Transfer of a Non-Newtonian Nanofluid in a Microtube, *Plos One, 7* (2012), 5, ID e37274
[20] Khalili, S., *et al.,* Unsteady MHD Flow and Heat Transfer Near Stagnation Point over a Stretching/Shrinking Sheet in Porous Medium Filled with a Nanofluid, *Chinese Phy., B, 23* (2014), 4, ID 048203
[21] Sheikholeslami, M., *et al*., Effects of Heat Transfer in Flow of Nanofluids over a Permeable Stretching Wall in a Porous Medium, *J. Comp. Theo. Nanosci., 11* (2014), 2, pp. 486-496
[22] Alsaedi, A., *et al.,* Effects of Heat Generation/Absorption on Stagnation Point Flow of Nanofluid over a Surface with Convective Boundary Conditions, *Comm. Nonlinear Sci. Num. Simul., 17* (2012), 11, pp. 4210-4223
[23] Khan, J. A., *et al.,* On Model for Three-Dimensional Flow of Nanofluid: An Application to Solar Energy, *J. Molecular Liquids, 194* (2014), June. pp. 41-47
[24] Crane, L. J., Flow Past a Stretching Plate, *J. Appl. Math. Phys. (ZAMP), 21* (1970), 4, pp. 645-647
[25] Mukhopadhyay, S., Slip Effects on MHD Boundary Layer Flow over an Exponentially Stretching Sheet with Suction/Blowing and Thermal Radiation, *Ain Shams Eng. J., 4* (2013), 3, pp. 485-491
[26] Bhattacharyya, K., *et al.,* Effects of Thermal Radiation on Micropolar Fluid Flow and Heat Transfer over a Porous Shrinking Sheet, *Int. J. Heat Mass Transfer, 55* (2012), 11-12, pp. 2945-2952
[27] Turkyilmazoglu, M., Exact Solutions for Two-Dimensional Laminar Flow over a Continuously Stretching or Shrinking Sheet in an Electrically Conducting Quiescent Couple Stress Fluid, *Int. J. Heat Mass Transfer, 72* (2014), May, pp. 1-8
[28] Turkyilmazoglu, M., A Note on Micropolar Fluid Flow and Heat Transfer over a Porous Shrinking Sheet, *Int. J. Heat and Mass Transfer, 72* (2014), May, pp. 388-391
[29] Sheikholeslami, M., *et al.,* Effects of Heat Transfer in Flow of Nanofluids over a Permeable Stretching Wall in a Porous Medium, *J. Comp. Theo. Nanosci., 11* (2014), 2, pp. 486-496

[30] Sheikholeslami, M., Ganji, D. D., Three Dimensional Heat and Mass Transfer in a Rotating System Using Nanofluid, *Powder Technology, 253* (2014), Feb., pp. 789-796
[31] Ibrahim, W., *et al.,* MHD Stagnation Point Flow and Heat Transfer due to Nanofluid towards a Stretching Sheet, *Int. J. Heat and Mass Transfer, 56* (2013), 1-2, pp. 1-9
[32] Malvandi, A., *et al.,* Slip Effects on Unsteady Stagnation Point Flow of a Nanofluid over a Stretching Sheet, *Powder Technology, 253* (2014), Feb., pp. 377-384
[33] Rashidi, M. M., *et al.,* Mixed Convection Heat Transfer for Viscoelastic Fluid Flow over a Porous Wedge with Thermal Radiation, *Adv. Mech. Eng., 2014* (2014), 10, ID 735939
[34] Farooq, U., *et al.,* Heat and Mass Transfer of Two-Layer Flows of Third-Grade Nanofluids in a Vertical Channel, *Appl. Mathe. Comp., 242* (2014), Sep., pp. 528-540
[35] Shehzad, S. A., *et al.,* Thermophoresis Particle Deposition in Mixed Convection Three-Dimensional Radiative Flow of an Oldroyd-B Fluid, *J. Taiwan Institute of Chemical Engineers, 45* (2014), 3, pp. 787-794
[36] Awais, M., *et al.,* Time-Dependent Three-Dimensional Boundary Layer Flow of a Maxwell Fluid, *Computers and Fluids, 91* (2014), Mar., pp. 21-27
[37] Hayat, T., *et al.,* MHD Axisymmetric Flow of Third Grade Fluid between Stretching Sheets with Heat Transfer, *Computers and Fluids, 86* (2013), Nov., pp. 103-108
[38] Turkyilmazoglu, M., Solution of the Thomas-Fermi Equation with a Convergent Approach, *Comm. Nonlinear Sci. Num. Simul., 17* (2012), 11, pp. 4097-4103
[39] Abbasbandy, S., *et al.,* On Convergence of Homotopy Analysis Method and Its Application to Fractional Integro-Differential Equations, *Quaestiones Math., 36* (2013), 1, pp. 93-105
[40] Aziz, A., A Similarity Solution for Laminar Thermal Boundary Layer over a Flat Plate with a Convective Surface Boundary Condition, *Comm. Non-linear Sci. Num. Simul., 14* (2009), 4, pp. 1064-1068
[41] Ishak, A., Similarity Solutions for Flow and Heat Transfer over a Permeable Surface with Convective Boundary Condition, *Appl. Math. Comp., 217* (2010), 2, pp. 837-842

Paper submitted: August 19, 2014
Paper revised: October 23, 2014
Paper accepted: November 04, 2014